Polarized optical reflectance and electronic band structure of α'-NaV_2O_5

V. C. Long, Z. Zhu, and J. L. Musfeldt
Department of Chemistry, State University of New York at Binghamton, Binghamton, New York 13902-6016

X. Wei
National High Magnetic Field Laboratory, Florida State University, Tallahassee, Florida 32306

H.-J. Koo and M.-H. Whangbo
Department of Chemistry, North Carolina State University, Raleigh, North Carolina 27596-8204

J. Jegoudez and A. Revcolevschi
Laboratoire de Chimie des Solides, Université de Paris-Sud, Bâtiment 414, F-91405 Orsay, France
(Received 16 July 1999)

We report polarized optical reflectance studies of α'-NaV_2O_5 between 0.5 and 6 eV as a function of temperature (T) and magnetic field (H). The electronic excitations and their polarization dependence are interpreted according to our extended Hückel tight-binding polarized band structure calculations. Strong bands near 1 eV in both chain and rung directions are attributed to V $d \rightarrow d$ transitions. Charge transfer excitations are estimated to begin near 3.3 eV and have significant strength at 4.4 eV and above. The reflectance ratios, $\Delta R(T) = R(T)/R(T=4\ \mathrm{K})$, measured at $H=0$ and 28 T, reveal broad polarization-dependent changes through the low temperature transition, T_c. Integrated intensities of ΔR features exhibit a second-order transition at 36 K in zero field and at 33 ± 1 K in high field, consistent with a spin-Peierls aspect to the phase transition. [S0163-1829(99)06347-X]

I. INTRODUCTION

After the discovery of a low temperature (T) spin-gapped phase in α'-NaV_2O_5,[1,2] this compound rapidly attracted interest as the second inorganic spin-Peierls (SP) material. More recently, structural studies[3–7] have called into question the assumed nature of the spin chains and SP dimers,[8–10] and the character of the low T transition is now controversial.[9–15] In the room temperature structure of α'-NaV_2O_5, vanadium ions have oxidation state $+4.5$ and form weakly-coupled ladder chains along the b crystal axis.[3–6] V d_{xy}-like orbitals [confirmed by NMR (Ref. 16)] interact strongly across the ladder rungs via the shared Op_y orbital,[3,8,17,18] resulting in one spin per VOV rung. Since interactions between adjacent spins are much greater within each ladder than between ladder chains,[3,8,9,17] the ladders behave like $S=1/2$ Heisenberg linear chains, as apparent in the magnetic susceptibility above 100 K.[1,19] The opening of a spin gap at the phase transition ($T_c \approx 35$ K) is accompanied by unit cell doubling in the a and b directions, and quadrupling in the c direction.[7,20] An NMR study by Ohama *et al.*[21] showed that the transition involves charge localization, creating V^{4+} and V^{5+} on distinct V sites. One candidate for the resulting charge order is a zig-zag arrangement, which diagonally pairs V^{4+} spins located on neighboring chains.[8–10,22–25] Such transverse coupling motivates a classification of α'-NaV_2O_5 as an unconventional spin-Peierls material.[8,9] According to a 15 K crystal structure study by Lüdecke *et al.*,[7] the low T phase of α'-NaV_2O_5 is more complicated, with alternating modulated and unmodulated ladder chains along the a-axis. A bond valence sum analysis of this structure[26] suggests a charge distribution of $V^{4.5+}$ in the unmodulated chains and V^{4+} and V^{5+} in the modulated chains, different from the aforementioned NMR results.[21]

Although several optical and electronic structure investigations have focused on α'-NaV_2O_5, disagreements remain in a number of areas. In the middle infrared (MIR) region, a broad continuum between ≈ 100 and 2000 cm^{-1} (0.01–0.25 eV) in the rung-polarized direction[27–29] is of disputed origin.[6,29] An electronic band near 1 eV[27,28] was interpreted by one set of authors as phonon-assisted $d \rightarrow d$ transitions localized on a V^{4+} site[27,29] and by others as charge transfer excitations between V^{4+} and V^{5+} on opposite sides of a rung.[28,30] The assignment of a strong 3 eV absorption as the O$p \rightarrow$ Vd charge transfer band[27] was supported by modified LDA calculations,[18,31] but we find evidence for the true absorption edge in higher energy structures. Calculations based on the recently redetermined 300 K crystal structure[4] show that the lowest-lying band of α'-NaV_2O_5 is half-filled.[3,8,17] The insulating nature of α'-NaV_2O_5 (Ref. 32) is produced by electron localization associated with electron-electron repulsion.[3,17,18,31] Estimated values of the insulating gap include O$p \rightarrow$ Vd charge transfer (CT) at 2.7 eV,[18] rung-to-rung hopping excitations at 0.7 eV,[3,17] and a $d \rightarrow d$ excitation gap at 0.6 eV.[31]

In order to probe the rich electronic structure of α'-NaV_2O_5, we have extended previous optical measurements[27–29] to higher energies, and to the low temperature and high magnetic field regimes. By combining our measurements with extended Hückel tight-binding band structure calculations,[33,34] we assign excitation features of the observed conductivity and provide a framework for understanding the polarization dependence of the optical results across a wide energy range (0.5–6 eV). To gain insight into

TABLE I. Exponents, ζ_i, and valence shell ionization potentials, H_{ii}, of Slater-type orbitals, χ_i, used for extended Hückel tight-binding calculations. H_{ii}'s are the diagonal matrix elements, $\langle\chi_i|H^{eff}|\chi_i\rangle$, where H^{eff} is the effective Hamiltonian. In our calculations of the off-diagonal matrix elements, $H_{ij}=\langle\chi_i|H^{eff}|\chi_j\rangle$, the weighted formula was used (see Ref. 43). c_1 and c_2 are the contraction coefficients used in the Slater-type orbitals.

Atom	χ_i	H_{ii}	ζ_i	c_1	$\zeta_{i'}$	c_2
V	$4s$	-8.81	1.697	1.0		
V	$4p$	-5.52	1.260	1.0		
V	$3d$	-11.0	5.052	0.3738	2.173	0.7456
O	$2s$	-32.0	2.688	0.7076	1.675	0.3745
O	$2p$	-14.8	3.694	0.3322	1.659	0.7448

the microscopic nature of the low T phase, we also examine changes in the electronic structure of α'-NaV_2O_5 across the phase transition by polarized reflectance ratio $[\Delta R(T)]$ measurements. Finally, since optical electronic structure studies are a demonstrated means of mapping out the $H-T$ phase diagram of SP materials,[35–37] we made high-field ($H=28$ T) measurements of $\Delta R(T)$ to determine the field dependence of T_c, a common signature of the SP transition.[38,39]

II. EXPERIMENTAL METHOD

Two high quality single crystals of α'-NaV_2O_5 were grown by the flux method[40] and had dimensions of $\approx 8\times 2\times 0.8$ mm^3, and $4\times 2.5\times 0.4$ mm^3 with the long direction identified as parallel to the chains (b-axis). Measurements of power reflectance (R) were performed on a Perkin-Elmer Lambda-900 optical spectrometer, covering the energy range 0.5–6 eV with resolution between 1 and 3 nm. This system was custom retrofit to accommodate a reflectance stage and cryostat, and spectra were collected at ≈ 10, 40, and 300 K. Glan-Thompson and Glan-Taylor polarizers were used to select the response parallel to the chain direction ($\mathbf{E}\|b$) or rung direction ($\mathbf{E}\|a$). The Kramers-Kronig (KK) extrapolations were made as a constant below 0.5 eV and as ω^{-2} above 5.7 eV.

Small changes in reflectance in the vicinity of the low T phase transition were studied by measuring the reflectance ratios, $\Delta R(T)=R(T)/R(T=4\ \text{K})$, at two constant fields, $H=0$ and 28 T. The sample was mounted in an exchange gas cryostat whose tail fit into the bore of a 30 T resistive magnet; the applied field was perpendicular to the ab plane of the crystal. A grating spectrometer, equipped with a CCD camera or germanium detector, covered the energy range 0.75–2.5 eV. A series of polaroid film polarizers was employed. $\Delta R(T)$ was measured in 1 K steps around T_c in the CCD detector range and at larger temperature steps in the lower frequency region of the slower Ge scanning detector.

Extended Hückel tight-binding band structure (EHTB) calculations for α'-NaV_2O_5 were carried out using the centrosymmetric room temperature crystal structure.[4] Our calculations employed double-zeta Slater type orbitals[41,42] for the $3d$ orbitals of vanadium and the $2s/2p$ orbitals of oxygen, as described in Ref. 8. The atomic parameters used in our study are listed in Table I.

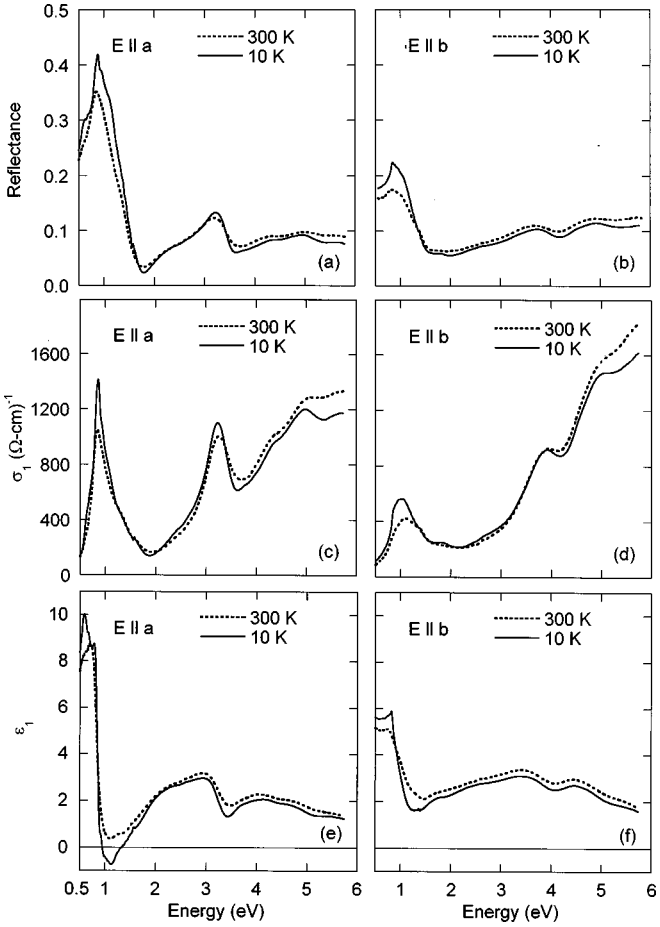

FIG. 1. Frequency-dependent reflectance (upper panels), conductivity (middle panels), and dielectric constant (lower panels) of α'-NaV_2O_5 in the $\mathbf{E}\|a$ and $\mathbf{E}\|b$ polarizations. The frequency is given in units of eV. The dotted line spectra were taken at ≈ 300 K and the solid line spectra at ≈ 10 K.

III. RESULTS AND DISCUSSION

A. Polarized optical conductivity and band structure

The top panels of Fig. 1 display the room temperature and ≈ 10 K reflectance of α'-NaV_2O_5 in both polarizations. The frequency-dependent conductivity, $\sigma_1(\omega)$, and dielectric constant, $\epsilon_1(\omega)$, determined by KK analysis, are shown in the lower panels. Both are characteristic of a highly anisotropic insulating material. In general, the lossy and dispersive features for the polarization along the rung direction ($\mathbf{E}\|a$) are more intense, better defined, and occur at slightly lower energies than those polarized in the chain direction ($\mathbf{E}\|b$). In $\sigma_1(\omega)$, we find strong low-energy electronic excitations centered around 1 eV (0.86 eV in $\mathbf{E}\|a$ and 1.1 eV in $\mathbf{E}\|b$), in good agreement with other $\sigma_1(\omega)$ results[28] and with transmittance and ellipsometry data at 300 K.[27,44,45] Following a reduced conductivity region in both polarizations, there occur well-defined excitations centered at 3.2 and 3.9 eV in $\mathbf{E}\|a$ and $\mathbf{E}\|b$, respectively. These are succeeded by broader overlapping bands centered at 4.4 and 5.0 eV in $\mathbf{E}\|a$ and by a band at 5.0 eV in $\mathbf{E}\|b$. The positive slope of $\sigma_1(\omega)$ above 5 eV implies the existence of additional higher energy excitations beyond the range of our measurements.

To analyze the observed room temperature conductivity of α'-NaV_2O_5, we examine its electronic band structure cal-

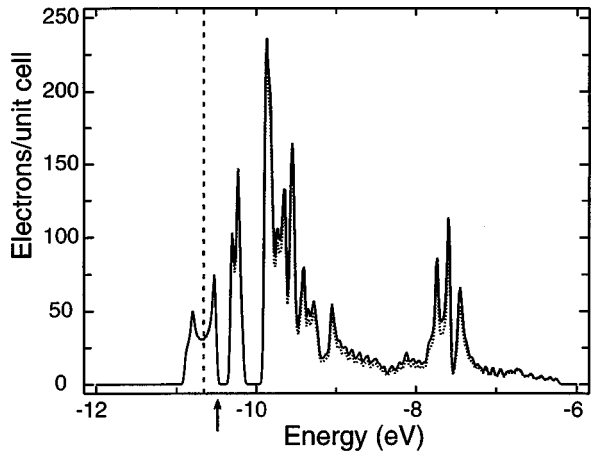

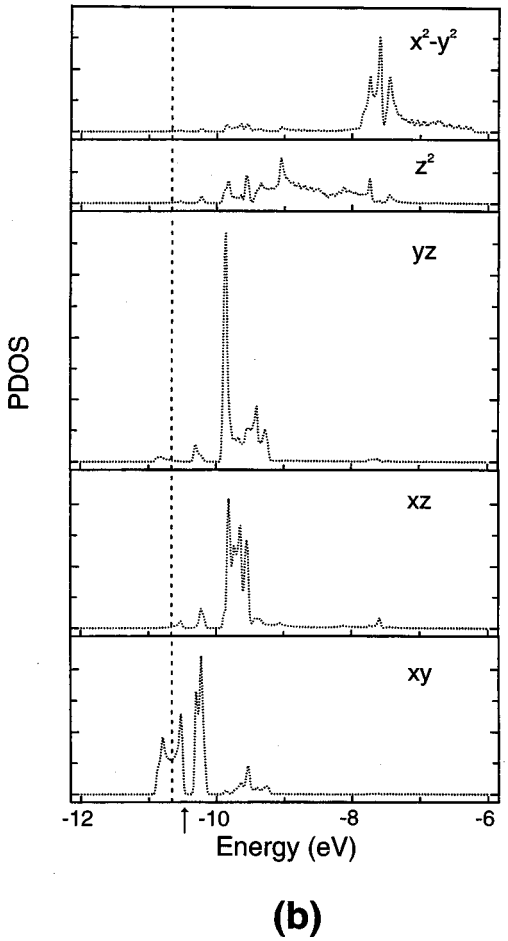

FIG. 2. (a) Density of states plots for the room temperature structure of α'-NaV_2O_5. The solid line refers to the total DOS and the dotted line to the PDOS for the V d orbitals. (b) PDOS plots calculated for the V d_{xy}, d_{xz}, d_{yz}, d_{z^2}, and $d_{x^2-y^2}$ orbitals. Each interval of the PDOS axis corresponds to 25 electrons per unit cell.

culated by the EHTB method. Figure 2(a) shows the total density of states (DOS) as a solid line and the projected density of states (PDOS) for the V d orbitals as a dotted line. For simplicity, only the region of d-block bands is shown; the O p block is centered near -17 eV. The PDOS plots for the individual V d orbitals, shown in Fig. 2(b), reveal that the

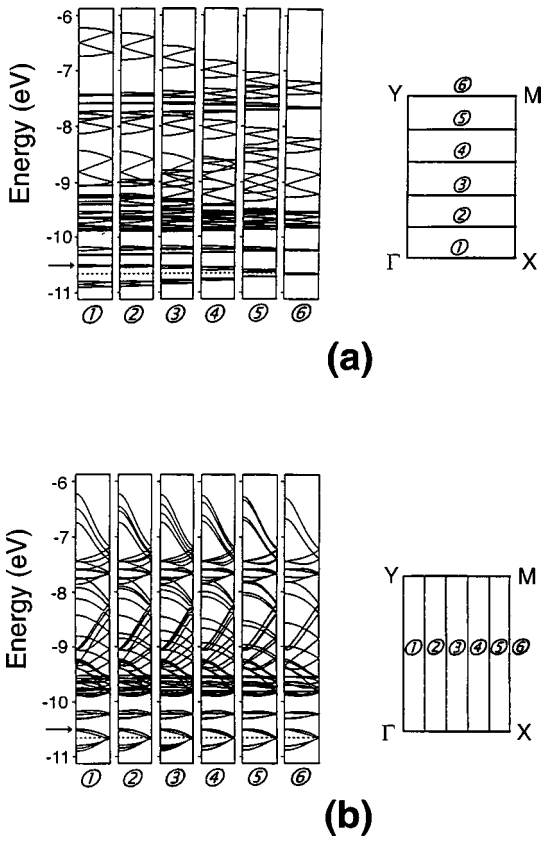

FIG. 3. Dispersion relations (left) calculated for the d-block bands of α'-NaV_2O_5 along the six wave vector lines (right) parallel to the a^* axis in (a) and parallel to the b^* axis in (b). In units of a^* and b^*, the symbols representing the positions of the Brillouin zone are defined as $\Gamma=(0,0)$, $X=(a^*/2,0)$, $M=(a^*/2,b^*/2)$, and $Y=(0,b^*/2)$.

d-block bands increase in energy as $d_{xy}<d_{xz}<d_{yz}<d_{z^2}<d_{x^2-y^2}$. This sequence is the same as for the isolated VO_5 square pyramid, the building block of the V-O lattice of α'-NaV_2O_5.[8] Overall features of the d-block bands are in good agreement with recent first principles calculations.[3,18,31] The d_{xy} bands are split in two because $V^{4.5+}$ ions interact strongly across each rung,[8] and as a result, the lower d_{xy} band becomes half-filled. The Fermi level (dashed line) of Figs. 2 and 3 was determined under the assumption that α'-NaV_2O_5 is a metal. The actual magnetic insulating state of α'-NaV_2O_5 (one spin per VOV rung) is represented by the electron configuration in which d_{xy}-band energy levels are singly occupied.[46,47] Thus, the Fermi level appropriate for this system is at the top of the lower d_{xy} band, as indicated by arrows in Figs. 2 and 3. Optical excitations between the various states can be divided into two main classes: those at energies $>\approx 4.4$ eV, which are O p-block$\rightarrow$V d-block transitions, and those $<\approx 4.4$ eV, which are transitions within the V d-block bands. Within the V d block, excitations can occur from the lower d_{xy} band (henceforth, denoted d_{xy}^+) to the upper d_{xy} band (d_{xy}^-) and from d_{xy}^+ to each of the higher energy V d orbitals.

In polarized reflectance measurements, the optical absorption involves occupied and unoccupied energy levels having the same wave vector aligned along the polarization direction.[48,49] To understand the polarization dependence of

$\sigma_1(\omega)$, we compare optical transitions polarized along the *a* axis (*b* axis) (Fig. 1) with the energy levels of *d*-block bands along wave vector lines parallel to the a^* (b^*) direction (Fig. 3). In general, DOS values increase with the flatness of the band, so electronic excitations are expected to be more intense in the rung than in the chain polarization, in good agreement with our conductivity data below ≈ 4 eV. The *d*-block bands are noticeably more dispersive in the chain direction [Fig. 3(b)] than in the rung direction [Fig. 3(a)] due to linear oxygen-vanadium linkages all along the chains. In the $\mathbf{E}\|b$ polarization, the character of $\sigma_1(\omega)$ between 1 and 4 eV is reminiscent of a one-dimensional (1D) band,[50] consistent with the greater band dispersion in this direction.

We assign electronic excitations in $\sigma_1(\omega)$ based on the DOS and band dispersion relations shown in Figs. 2 and 3. Within the V *d* block, we expect to see fairly sharp features due to the localized nature of such excitations. The intense features near 1 eV are assigned as $d_{xy}^{+} \rightarrow d_{xz}$ and $d_{xy}^{+} \rightarrow d_{yz}$ transitions. The weak sidebands of the ≈ 1 eV features are expected due to fine structure in the density of states. The calculated $d_{xy}^{+} \rightarrow d_{xy}^{-}$ transition is centered near 0.5 eV with an onset of ≈ 0.2 eV. As pointed out by Popova *et al.*,[29] this excitation will be polarized in the rung direction, according to a symmetry analysis of the idealized VOV rung within the C_{2v} point group.[51] In the $\mathbf{E}\|a$ conductivity, the features closest in energy to the calculated transition are the MIR electronic band[27,28] and a low energy shoulder (0.64 eV) of the $d_{xy}^{+} \rightarrow d_{xz}$ and $d_{xy}^{+} \rightarrow d_{yz}$ band. Since each of these has minimal overlap with the predicted range, we cannot positively identify the $d_{xy}^{+} \rightarrow d_{xy}^{-}$ excitations in $\sigma_1(\omega)$. The second strong conductivity band at 3.2 eV in the *a* direction (Fig. 1) is assigned as a $d_{xy}^{+} \rightarrow d_{x^2-y^2}$ excitation. The 3.9 eV feature along *b* may also be related to the $d_{xy}^{+} \rightarrow d_{x^2-y^2}$ excitation, since the dispersion of the $d_{x^2-y^2}$-block band is 1D-like and the DOS should therefore be high at the top of this band. The PDOS of the d_{z^2} band is wide and reduced in magnitude compared to the rest of the V *d* block, which explains the lower $\sigma_1(\omega)$ between ≈ 1.6 and 2.3 (2.6) eV in $\mathbf{E}\|a$ ($\mathbf{E}\|b$).

Charge transfer transitions from the top of the O *p* block to the bottom of the V *d* block constitute the main energy gap in α'-NaV_2O_5, and a series of broad overlapping features is observed in both polarizations of $\sigma_1(\omega)$ above ≈ 4 eV. First maxima in the CT excitations occur at 4.4 and 5.0 eV along *a* and *b*, respectively. Using a linear extrapolation of the steepest leading edge of the absorption, we assign the optical gap to be ≈ 3.3 (3.5) eV in the rung (chain) polarization, in reasonable agreement with the EHTB calculations (4.4 eV), assuming normal broadening of the gap.[52] This gap value should be distinguished from a previous 3 eV gap assignment,[27] which referred to bands that we identify (based on a wider spectral range) as V $d_{xy} \rightarrow d_{x^2-y^2}$, a totally different type of excitation. The polarized band structures do not account for the fact that $\mathbf{E}\|b$ CT transitions have greater intensity than the $\mathbf{E}\|a$ transitions and in fact, predict the reverse. Calculation of transition moments might help explain this discrepancy.

The temperature dependence of $\sigma_1(\omega)$ between room temperature and 10 K is shown in the middle panels of Fig. 1. In both polarizations, the $d \rightarrow d$ bands become slightly sharper and more intense with decreasing *T*, nearly all of the change occurring above T_c [at the scale shown, $\sigma_1(\omega)$ at 10 K looks virtually identical to $\sigma_1(\omega)$ at 40 K]. This contrasts markedly with the reduced oscillator strength of Cu^{2+} $d \rightarrow d$ transitions in $CuGeO_3$ at low *T*,[35] which is due to the phonon-assisted nature of those transitions.[53,54] On the other hand, there appears to be a decrease in intensity of the overlapping CT bands with decreasing *T* (although the proximity of these features to the KK extrapolation makes this conclusion less reliable). The resulting shift of spectral weight to the lower energy localized excitations is consistent with the approach of a charge ordering transition, producing an increased localization of charge on vanadium sites.

We point out that the V $d \rightarrow d$ transitions described in the present work are on-rung excitations, chiefly localized within the VO_5 square pyramid. Furthermore, in the relevant C_{2v} symmetry of the idealized rung,[29] the $A_2 \rightarrow B_1$ and $A_2 \rightarrow B_2$ transitions, which characterize the ≈ 1 eV $d_{xy}^{+} \rightarrow d_{xz}$ and $d_{xy}^{+} \rightarrow d_{yz}$ excitations, are both symmetry allowed.[51,55] Thus, our model of on-rung excitations should be differentiated from previous interpretations of the ≈ 1 eV bands, such as rung-to-rung hopping,[3] across-the-rung hopping,[28] and phonon-assisted $d \rightarrow d$ transitions on a V^{4+} site.[27,29] On-rung excitations tend to have higher overlap amplitudes, and provide a better explanation for the strong spectral intensity than the aforementioned hopping or phonon-assisted transitions.

B. Electronic structure changes at the transition

Figure 4 displays the zero-field reflectance ratios (ΔR) determined for α'-NaV_2O_5 in both *a* and *b* polarizations. These look nearly identical to the high-field (28 T) reflectance ratios (not shown). Consistent with the power reflectance of α'-NaV_2O_5, ΔR is strongly polarization-dependent. Changes in ΔR occur in wide energy bands centered at different energies in rung and chain directions. This behavior is distinct from that of $CuGeO_3$, in which ΔR features are narrower and appear near the same energy in both polarizations.[35] These differences indicate stronger one-dimensionality and a greater modification of the electronic structure of α'-NaV_2O_5 at the phase transition, in accord with the charge ordering aspect of that transition, compared to weaker changes associated with the magneto-elastic transition in $CuGeO_3$. The insets to Fig. 4 show that integrated intensities of the ΔR bands yield a similar *T* dependence in both polarizations, the gradual nature of which is typical of a second-order transition. This second-order behavior is consistent with either a spin-Peierls transition[56] or an order-disorder transition, such as may occur due to charge fluctuations.[57] The similar appearances of zero-field and high-field integrated intensities confirm that the second-order character of the transition is unchanged up to 28 T. To our knowledge, this magnitude of magnetic field is higher than any previously investigated in this compound.[58]

An important signature of the SP phase transition is the magnetic field (*H*) dependence of T_c,[38,39] which is known to follow a quadratic behavior in *H* below a critical field, H_c. The usual mean-field relation,[56] $H_c \approx 1.5 k_B T_c / g\mu_B$, yields $H_c \approx 40$ T, well above the field applied in these experiments. Here, $g = 1.938$ for $H\|c$ axis.[59] T_c, determined from the ''knee'' of the integrated intensity versus *T* (insets to Fig. 4), is reduced from ≈ 36 K at zero field to $\approx 33 \pm 1$ K at

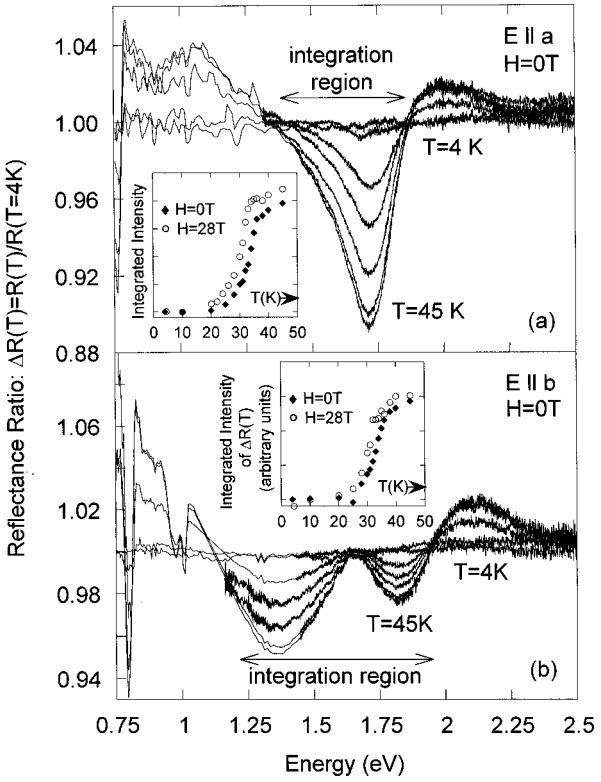

FIG. 4. Temperature dependence of zero-field reflectance ratios, ΔR, for the (a) $\mathbf{E}\|a$ and (b) $\mathbf{E}\|b$ polarizations. At the center of the spectra, the temperatures are, from top to bottom: $T=4$, 10, 20, 30, 35, 40, 45 K; at the low energy end, from bottom to top: $T=4$, 20, 30, 40, 45 K. The inset for each polarization shows the integrated intensities of the ΔR features versus temperature, with the integration region shown by arrows in the main figure. Empty circles refer to the zero-field data and solid diamonds to the data taken at $H=28$ T (not shown).

$H=28$ T. According to standard theory, the transition temperature of a SP system obeys $T_c(H)/T_c(0)=1-\alpha[g\mu_B H/2k_B T_c(0)]^2$, with the prefactor, α, equal to 0.44 or 0.364.[38,39] We find $0.22<\alpha<0.42$, which overlaps well with the expected range and allows for a possible quadratic field dependence of T_c, in contrast with previous determinations of α which were as much as an order of magnitude smaller than expected.[15,60] In sum, our ΔR results for α'-NaV_2O_5 are consistent with a conventional SP transition, as manifest in the second-order character and field dependence of T_c. The fact that in many other regards α'-NaV_2O_5 does not conform to current understanding of an ordinary spin-Peierls system[8,15,21,32,59,61,62] clearly motivates further high-field studies of this complex material.

To gain additional insight into the electronic structure changes occurring at T_c, we have calculated $\sigma_1(\omega)$ at $T=40$ K for comparison with $\sigma_1(\omega)$ at 10 K, as shown in Fig. 5. For this purpose, we combined our 10 K power reflectance spectrum with the reflectance ratio $\Delta R(40\ \mathrm{K})=R(40\ \mathrm{K})/R(4\ \mathrm{K})$ and made a KK analysis of the resulting spectrum.[63] Although the minute changes in $\sigma_1(\omega)$ (inset to Fig. 5) might be suspect if derived from the difference in the power reflectance, their origin in the reproducible trends of the reflectance ratios assures that they are real. As α'-NaV_2O_5 moves into the low T phase, the low-energy

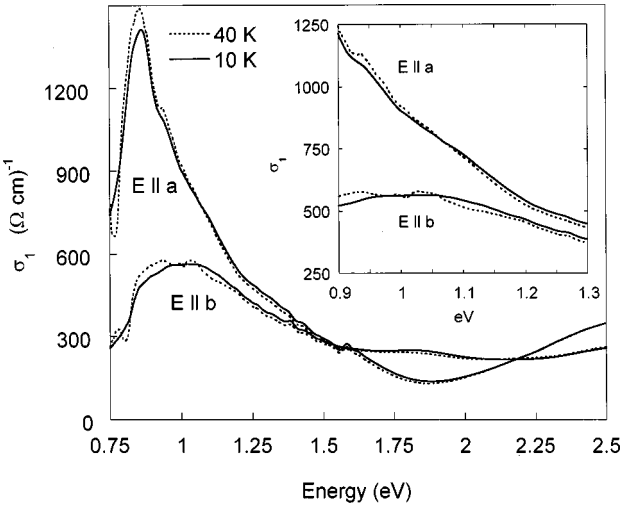

FIG. 5. Frequency-dependent conductivity at $T\approx 10$ K (solid line) and ≈ 40 K (dotted line) in both polarizations. Inset shows magnification of region where the two temperature spectra cross.

bands of both polarizations show a decrease in spectral weight below ≈ 1.06 eV and an increase in weight in the high-energy tails of the same bands. We deduce that the $d^+_{xy}\rightarrow d_{xz}$ and $d^+_{xy}\rightarrow d_{yz}$ excitations shift to slightly higher energy in the low-temperature phase. A challenge for future band structure calculations of the low temperature structure of α'-NaV_2O_5 will be to reproduce and explain the blue shifts of these excitations.

IV. CONCLUSION

In summary, we report polarized optical reflectance studies of α'-NaV_2O_5 between 0.5 and 6 eV as a function of temperature and magnetic field. Electronic excitations determined by EHTB electronic band structure calculations are in good overall agreement with the observed zero-field optical conductivity. Greater oscillator strength in the rung compared to the chain polarization is consistent with *d*-block bands that are less dispersive along the rung direction. The strong frequency-dependent conductivity bands near 1 eV are associated with on-rung $d^+_{xy}\rightarrow d_{xz}$ and $d^+_{xy}\rightarrow d_{yz}$ transitions. $Op\rightarrow Vd$ charge transfer excitations are calculated to begin at ≈ 4.4 eV, in reasonable agreement with the experimental optical gap, which is estimated at ≈ 3.3 (3.5) eV in the rung (chain) direction, and with above-gap transitions gaining significant strength near 4.4 (5.0) eV. Reflectance ratios, ΔR, measured in chain and rung directions, reveal broad polarization-dependent changes through the 36 K phase transition. Integrated intensities of the ΔR features as a function of T show a second-order type phase transition at both zero field and high field, and a ≈ 3 K reduction in T_c at 28 T, consistent with a possible quadratic field dependence of T_c.

ACKNOWLEDGMENTS

Work at the State University of New York at Binghamton and at North Carolina State University was supported by the Division of Materials Science, Basic Energy Sciences at the

U.S. Department of Energy under Grants Nos. DE-FG02-99ER45741 and DE-FG05-86ER45259, respectively. Some of these measurements were performed at the National High Magnetic Field Laboratory in Tallahassee, Florida, which is supported by NSF Cooperative Agreement No. DMR-9527035 and by the State of Florida. We thank Andrei Sushkov and Andrea Damascelli for careful readings of the manuscript.

[1] M. Isobe and Y. Ueda, J. Phys. Soc. Jpn. **65**, 1178 (1996).
[2] M. Weiden, R. Hauptmann, C. Geibel, F. Steglich, M. Fischer, P. Lemmens, and G. Güntherodt, Z. Phys. B **103**, 1 (1997).
[3] H. Smolinski, C. Gros, W. Weber, U. Peuchert, G. Roth, M. Weiden, and C. Geibel, Phys. Rev. Lett. **80**, 5164 (1998).
[4] H. G. von Schnering, Y. Grin, M. Kaupp, M. Somer, R. K. Kremer, O. Jepsen, T. Chatterji, and M. Weiden, Z. Kristallogr. **213**, 246 (1998).
[5] T. Chatterji, K. D. Liss, G. J. McIntyre, M. Weiden, R. Hauptmann, and C. Geibel, Solid State Commun. **108**, 23 (1998).
[6] A. Meetsma, J. L. de Boer, A. Damascelli, T. T. M. Palstra, J. Jegoudez, and A. Revcolevschi, Acta Crystallogr., Sect. C: Cryst. Struct. Commun. **C54**, 1558 (1998).
[7] J. Lüdecke, A. Jobst, S. van Smaalen, E. Morré, C. Geibel, and H.-G. Krane, Phys. Rev. Lett. **82**, 3633 (1999).
[8] H.-J. Koo and M.-H. Whangbo, Solid State Commun. **111**, 353 (1999).
[9] H. Seo and H. Fukuyama, J. Phys. Soc. Jpn. **67**, 2602 (1998).
[10] M. V. Mostovoy and D. I. Khomskii, cond-mat/9806215 (unpublished).
[11] P. Thalmeier and P. Fulde, Europhys. Lett. **44**, 242 (1998).
[12] S. Nishimoto and Y. Ohta, J. Phys. Soc. Jpn. **67**, 2996 (1998).
[13] A. N. Vasil'ev, V. V. Pryadun, D. I. Khomskii, G. Dhalenne, A. Revcolevschi, M. Isobe, and Y. Ueda, Phys. Rev. Lett. **81**, 1949 (1998).
[14] M. Köppen, D. Pankert, R. Hauptmann, M. Lang, M. Weiden, C. Geibel, and F. Steglich, Phys. Rev. B **57**, 8466 (1998).
[15] W. Schnelle, Yu. Grin, and R. K. Kremer, Phys. Rev. B **59**, 73 (1999).
[16] T. Ohama, H. Yasuoka, M. Isobe, and Y. Ueda, J. Phys. Soc. Jpn. **66**, 3008 (1997).
[17] P. Horsch and F. Mack, Eur. Phys. J. B **5**, 367 (1998).
[18] Z. S. Popović and F. R. Vukajlović, Phys. Rev. B **59**, 5333 (1999).
[19] F. Mila, P. Millet, and J. Bonvoisin, Phys. Rev. B **54**, 11 925 (1996).
[20] Y. Fujii, H. Nakao, T. Yosihama, M. Nishi, K. Nakajima, K. Kakurai, M. Isobe, Y. Ueda, and H. Sawa, J. Phys. Soc. Jpn. **66**, 326 (1997).
[21] T. Ohama, H. Yasuoka, M. Isobe, and Y. Ueda, Phys. Rev. B **59**, 3299 (1999).
[22] C. Gros and R. Valenti, Phys. Rev. Lett. **82**, 976 (1999).
[23] J. Riera and D. Poilblanc, Phys. Rev. B **59**, 2667 (1999).
[24] A. I. Smirnov, M. N. Popova, A. B. Sushkov, S. A. Golubchik, D. I. Khomskii, M. V. Mostovoy, A. N. Vasil'ev, M. Isobe, and Y. Ueda, Phys. Rev. B **59**, 14 546 (1999).
[25] H. Schwenk, S. Zherlitsyn, B. Lüthi, E. Morre, and C. Geibel, Phys. Rev. B **60**, 9194 (1999).
[26] H.-J. Koo and M.-H. Whangbo (unpublished).
[27] S. A. Golubchik, M. Isobe, A. N. Ivlev, B. N. Mavrin, M. N. Popova, A. B. Sushkov, Y. Ueda, and A. N. Vasil'ev, J. Phys. Soc. Jpn. **66**, 4042 (1997); **68**, 318 (1999).
[28] A. Damascelli, D. van der Marel, M. Grüninger, C. Presura, and T. T. M. Palstra, Phys. Rev. Lett. **81**, 918 (1998).
[29] M. N. Popova, A. B. Sushkov, S. A. Golubchik, M. N. Mavrin, V. N. Denisov, B. Z. Malkin, A. I. Iskhakova, M. Isobe, and Y. Ueda, J. Exp. Theor. Phys. **88**, 1186 (1999).
[30] S. Nishimoto and Y. Ohta, J. Phys. Soc. Jpn. **67**, 3679 (1998).
[31] H. Wu and Q.-Q. Zheng, Phys. Rev. B **59**, 15 027 (1999).
[32] J. Hemberger, M. Lohmann, M. Nicklas, A. Loidl, M. Klemm, G. Obermeier, and S. Horn, Europhys. Lett. **42**, 661 (1998).
[33] M.-H. Whangbo and R. Hoffman, J. Am. Chem. Soc. **100**, 6093 (1978).
[34] Our calculations were carried out by employing the CAESAR program package (J. Ren, W. Liang, and M.-H. Whangbo, *Crystal and Electronic Structure Analysis Using CAESAR*, 1998. This book can be downloaded free of charge from the website http://www.PrimeC.com/.).
[35] V. C. Long, J. L. Musfeldt, T. Schmiedel, A. Revcolevschi, and G. Dhalenne, Phys. Rev. B **56**, 14 263 (1997).
[36] V. C. Long, Z. Zhu, J. L. Musfeldt, T. Schmiedel, X. Wei, A. Revcolevschi, and G. Dhalenne (unpublished).
[37] J. Zeman, G. Martinez, P. H. M. van Loosdrecht, G. Dhalenne, and A. Revcolevschi, Phys. Rev. Lett. **83**, 2648 (1999).
[38] L. N. Bulaevskii, A. I. Buzdin, and D. I. Khomskii, Phys. Rev. B **27**, 5 (1978).
[39] M. C. Cross, Phys. Rev. B **20**, 4606 (1979).
[40] M. Isobe, C. Kagami, and Y. Ueda, J. Cryst. Growth **181**, 314 (1997).
[41] E. Clementi and C. Roetti, At. Data Nucl. Data Tables **14**, 177 (1974).
[42] A. D. McLean and R. S. McLean, At. Data Nucl. Data Tables **26**, 197 (1981).
[43] J. Ammeter, H.-B. Bürgi, J. C. Thibeault, and R. Hoffman, J. Am. Chem. Soc. **100**, 3686 (1978).
[44] P. H. M. van Loosdrecht (unpublished).
[45] Although the magnitude of our $\sigma_1(\omega)$ is in good agreement with Ref. 28, our absorption coefficient (α) derived from KK analysis is 4–5 times higher than that of Refs. 27 and 44.
[46] M.-H. Whangbo, J. Chem. Phys. **70**, 4963 (1979).
[47] M.-H. Whangbo, J. Chem. Phys. **73**, 3854 (1980).
[48] H.-J. Koo, M.-H. Whangbo, J. Dong, I. Olejniczak, J. L. Musfeldt, J. A. Schlueter, and U. Geiser, Solid State Commun. **112**, 403 (1999).
[49] Z. Zhu, S. Chowdhary, V. C. Long, J. L. Musfeldt, X. Wei, H.-J. Koo, M.-H. Whangbo, H. Negishi, M. Inoue, J. Sarrao, and Z. Fisk (unpublished).
[50] S. Roth, *One Dimensional Metals: Physics and Materials Science* (VCH, New York, 1995), p. 69.
[51] Such a symmetry analysis was not fully consistent with other band assignments and we conclude that local distortions or crystal field effects perturb the C_{2v} symmetry, resulting in more allowed transitions than in the idealized case.
[52] R. H. McKenzie and J. W. Wilkins, Phys. Rev. Lett. **69**, 1085 (1992).

[53] M. Bassi, P. Camagni, R. Rolli, and G. Samoggia, Phys. Rev. B **54**, 11 030 (1996).

[54] M. N. Popova, A. B. Sushkov, S. A. Golubchik, A. N. Vasil'ev, and L. I. Leonyuk, Zh. Éksp. Teor. Fiz. **83**, 2230 (1996) [JETP **83**, 1227 (1996)].

[55] P. W. Atkins, *Physical Chemistry, Second Edition* (W. H. Freeman and Company, San Francisco, 1982), p. 545.

[56] J. W. Bray, L. V. Interrante, I. S. Jacobs, and J. C. Bonner, in *Extended Linear Chain Compounds*, edited by J. S. Miller (Plenum, New York, 1983), Vol. 3, p. 353.

[57] S. Nishimoto and Y. Ohta, J. Phys. Soc. Jpn. **67**, 4010 (1998).

[58] We were informed recently that a magnetic torsion experiment up to $H=28$ T has been made on α'-NaV_2O_5. [P. H. M. van Loosdrecht (private communication).]

[59] A. N. Vasil'ev, A. I. Smirnov, M. Isobe, and Y. Ueda, Phys. Rev. B **56**, 5065 (1997).

[60] P. Fertey, M. Poirier, M. Castonguay, J. Jegoudez, and A. Revcolvschi, Phys. Rev. B **57**, 13 698 (1998).

[61] D. Smirnov, P. Millet, J. Leotin, D. Poilblanc, J. Riera, D. Augier, and P. Hansen, Phys. Rev. B **57**, 11 035 (1998).

[62] S. Ravy, J. Jegoudez, and A. Revcolevschi, Phys. Rev. B **59**, 681 (1999).

[63] Note that since ΔR changes negligibly between 4 K and 10 K (see Fig. 4), this method provided us with an approximation of $\sigma_1(\omega)$ at 40 K which could be compared to $\sigma_1(\omega)$ at 10 K, without additional errors introduced by normalizing to a reference mirror.